ISSN: 2579-5821 (Print)
ISSN: 2579-5546 (Online)
URL address: http://journal.unhas.ac.id/index.php/geocelebes
DOI: 10.70561/geocelebes.v10i1.49005

Jurnal Geocelebes Vol. 10 No. 1, April 2026, 69 – 81

Identification of Magma Intrusion Distribution in the Sekincau Mountain Area Based on the Euler Deconvolution Method of Gravity Data

Anisa Amanda*, Rizki Buana Agustian, Aksela Dian Fista, Ilham Dani

Geophysical Engineering, University of Lampung, Bandar Lampung, 35145, Indonesia.

*Corresponding author. Email: anisaamanda2803@gmail.com

Manuscript received: 17 December 2025; Received in revised form: 26 January 2026; Accepted: 27 March 2026

Abstract

Mount Sekincau, West Lampung, is located within the active Bukit Barisan tectonic zone and exhibits geothermal potential controlled by magmatic activity and geological structures. This study aims to identify the distribution and depth of magmatic intrusions using gravity data analysis and Euler deconvolution. GGMPlus satellite gravity data were processed to generate Complete Bouguer Anomaly, regional and residual anomalies, analytical signal, Euler solutions, and three-dimensional models. The Complete Bouguer Anomaly values range from 38.05 to 58.32 mGal, with high anomalies concentrated in the central part of the study area. Positive residual anomalies ranging from 0.88 to 2.78 mGal indicate the presence of shallow high-density bodies interpreted as magmatic intrusions. Analytical signal and Euler deconvolution results with a structural index of 0 reveal clusters of shallow sources associated with fault zones. Three-dimensional modeling confirms a southeastward-oriented intrusive body. These results indicate that shallow magmatic intrusions act as the primary heat source of the Sekincau geothermal system.

Keywords: Bouguer Anomaly; Euler Deconvolution; Geothermal; Gravity; Magma Intrusion.

Citation: Amanda, A., Agustian, R. B., Fista, A. D., & Dani, I. (2026). Identification of Magma Intrusion Distribution in the Sekincau Mountain Area Based on the Euler Deconvolution Method of Gravity Data. *Jurnal Geocelebes*, 10(1): 69–81, doi: 10.70561/geocelebes.v10i1.49005

Introduction

Mount Sekincau, located in West Lampung Regency, is situated within the active Bukit Barisan tectonic belt, which is characterized by volcanic activity, active faulting, and geothermal manifestations. The complex subsurface geological conditions in this area indicate the possible presence of shallow magmatic intrusions acting as the primary heat source of the geothermal system. However, the spatial distribution and depth of these intrusions remain poorly constrained. Therefore, this study aims to identify the distribution and depth of magmatic intrusions beneath Mount Sekincau using gravity data analysis. Specifically, this research focuses on separating the Complete Bouguer Anomaly (CBA) into regional and residual components and applying the Euler deconvolution method to estimate the geometry and depth of high-density anomaly sources interpreted as magmatic intrusions.

The gravity method is highly sensitive to lateral and vertical variations in subsurface rock density (Nurul et al., 2020). Conventional gravity surveys are commonly conducted using ground-based measurements, which provide high accuracy but are spatially limited and dependent on field accessibility. In contrast, Global Gravity Models (GGMs) integrate satellite gravimetry, terrestrial gravity data, and global topographic models, enabling uniform spatial coverage and consistent resolution over large areas. As a result, GGMs are particularly suitable for regional-scale geological studies and preliminary geothermal investigations.

With advancements in data acquisition and processing techniques, gravity surveys have been widely applied not only in hydrocarbon and mineral exploration (Dianwiyono & Wiradito, 2025; Raja et al., 2025; Alfuqara et al., 2025; Karaiskos et al., 2024), but also in delineating subsurface fault structures (Farrasha et al., 2023; Dani et al., 2024), mapping sedimentary cover (Zaenudin et al., 2020; Juwita et al., 2024; Ramadhani et al., 2025), reconstructing paleovolcanic facies (Nuzula et al., 2023), assessing geothermal systems (Sugianto et al., 2017), and identifying magmatic intrusions (Hosseini et al., 2025).

The interpretation of gravity data relies on gravity anomalies that reflect variations in subsurface rock density. The key parameter commonly used in gravity studies is the CBA, which represents the difference between observed and theoretical gravity values after applying latitude, free-air, Bouguer slab, and terrain corrections. The CBA is widely used to enhance subsurface density contrasts and to minimize non-geological effects in gravity data interpretation (Syukri, 2020). Bouguer gravity anomalies reflect the combined effects of both shallow and deep geological structures (Hasanah et al., 2016; Dung et al., 2025). To distinguish deep-seated regional structures from shallow local sources, gravity anomalies are commonly separated into regional and residual components (Supriyadi et al., 2019).

High gravity anomaly values indicate the presence of dense subsurface materials, such as magmatic intrusions or compact volcanic rocks, whereas low gravity anomalies represent low-density materials, including sedimentary deposits or hydrothermally altered zones (Liana et al., 2020; Zhanakulova et al., 2025).

Euler deconvolution is a semi-automatic interpretation method used to estimate the location and depth of subsurface anomaly sources based on potential field data. The integration of gravity anomaly modeling with Euler deconvolution enhances the interpretation of subsurface structures by enabling three-dimensional analysis through both deterministic and probabilistic approaches. (Castro et al., 2020; Cao et al., 2024; Nyakundi et al., 2025). Recently, modifications within methodologies such as improved Euler solution filtering through edge detection methods, the β-Vertical Derivative of Residual (β-VDR) approach, and Euler inversion have allowed a clearer understanding of complicated potential field information (Pham et al., 2024; Uieda, 2025). Despite these methodological advances, the application of gravity-based approaches combined with Euler deconvolution in the Sekincau Mountain area remains limited. Therefore, this study aims to separate regional and residual gravity anomalies and to analyze local anomaly patterns using Euler deconvolution to estimate subsurface geological structures.

Materials and Methods

The study area is in Sekincau District, West Lampung Regency, Lampung Province, Indonesia. Geographically, it extends from 5°02′50″ S to 5°10′25″ S and from 104°16′50″ E to 104°25′50″ E. The regional geology of the study area (Figure 1) is dominated by volcanic lithologies. The Hulusimpang Formation (Tomh) consists mainly of volcanic breccia, lava, and tuff. Overlying this unit is the Ranau Formation (Qtr), which is composed predominantly of pumice breccia and volcanic tuff. Additional volcanic units associated with the Barisan Zone include Quaternary volcanic rocks (Qv), characterized by andesite–basaltic lava, volcanic tuff, and volcanic breccia. The Young Quaternary Volcanic Rocks (Qhv) comprise breccia, lava, and volcanic tuff, while the Sekincau Young Quaternary Volcanic Rock Unit (Qvs) is primarily exposed along slope areas (Amin et al., 1994).

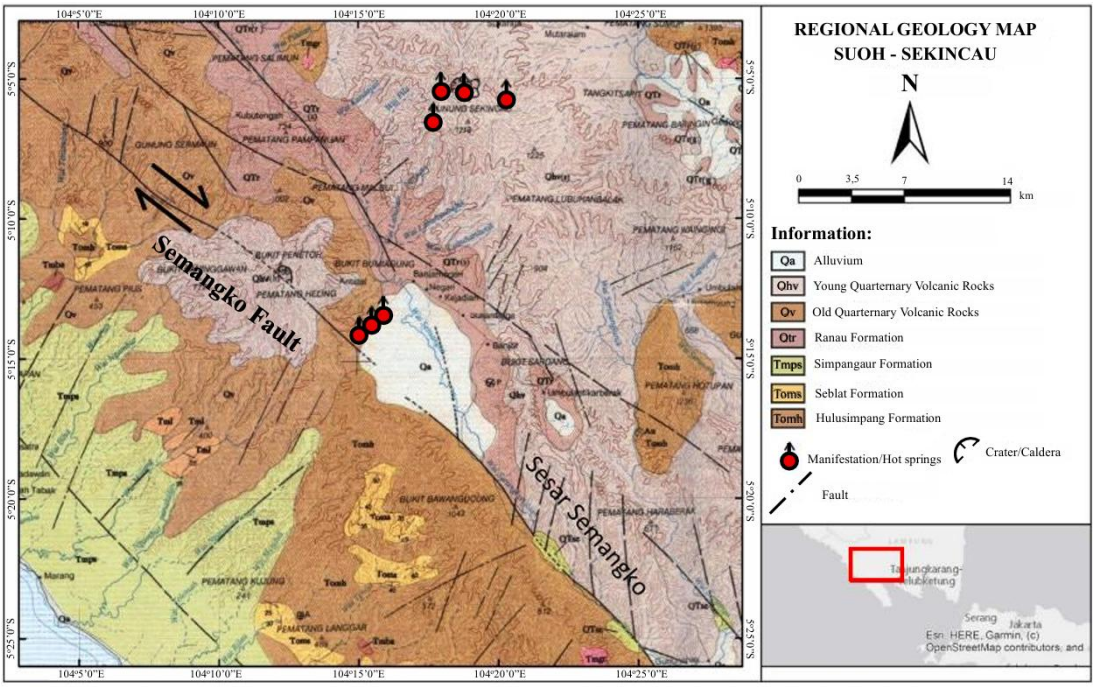

Figure 1. Geological Map of the Study Area (Iqbal & Juliarka, 2019).

The dataset used in this research is the 2013 Global Gravity Model Plus (GGMPlus) satellite gravity data with a high resolution of 7.2 arc seconds, or approximately 220 meters. The GGMPlus gravity model arose through a combination of EGM2008, gravity gradients from the European satellite mission Goce, and SRTM topography data, which allowed a short wavelength gravity signature to be detected, not accounted for in other standard satellite gravity models (Hirt et al., 2013). The SRTM topography data was used to provide a high level of topography detail to make possible accurate gravity modeling.

The first step in the processing is to compute the Bouguer anomaly using the GGMPlus gravity grid. As a prerequisite before computation, a thorough investigation is conducted on the data to remove any presence of outliers, missing data, or other numerical errors. The gravity anomaly is obtained by subtracting the theoretical gravity from the observed gravity. The observed gravity measurements are adjusted for tides and instrumental errors, and the theoretical gravity is calculated using the normal gravity model gṄ from the GRS80 ellipsoid model (Moritz, 1980). Proceeding further, corrections are applied with respect to Free Air (FAC), Bouguer (BC), and Topography (TERR). The methodology and equations employed in this study follow those outlined in Handyarso & Mauluda (2018), specifically Equations (1) through (6).

$$g_{\text{anomaly}} = g_{\text{observed}} - g_{\text{theoretical}} \quad (1)$$

$$g_{\text{observed}} = g_{read} + \text{tide} - \text{drift} \quad (2)$$

$$g_{\text{theoretical}} = g_n - \text{FAC} + \text{BC} - \text{TERR} \quad (3)$$

$$g_n = g_e \frac{1 + 0.00193185138639 \sin^2 \varphi}{\sqrt{1 - 0.00669437999013 \sin^2 \varphi}} \quad (4)$$

$$\text{FAC} = h \times (0.308 \frac{\text{mGal}}{\text{m}}) \quad (5)$$

$$\text{BC} = 2\pi \times \rho \times G \times h = 0.0419 \times \rho \times h \quad (6)$$

Description:

g_n : normal gravity value based on the World Geodetic System 1984 (mGal)

g_e : gravity at the equator (978032.67714 mGal)

g_{obs} : observed gravity value (mGal)

g_{read} : measured gravity value (mGal)
φ : latitude of measurement point (rad)
FAC : free air correction (mGal)
h : height of measurement point above mean sea level (m)
BC : bouguer correction (mGal)
TERR : field correction (mGal)
ρ : bouguer plate density (g/cm^3)
G : gravitational constant (Nm^2/kg^2)

Having obtained the Bouguer anomaly, we can separate it into a regional part and a residual part. For this separation, a moving average technique is used since it can emphasize regional characteristics with a high wavelength and suppress local variations with a short wavelength associated with shallow geology. To achieve this, a regional gravity anomaly is computed by averaging a series of consecutive gravity anomaly data points, and a residual is obtained by subtracting a regional anomaly from a Bouguer anomaly. A one-dimensional moving average can be performed using the following formula (Ramadhan & Pohan, 2024):

$$\Delta T_{reg}(i,j) = \left(\frac{1}{N}\right).\ (\Delta T(i-n, j-n) + \cdots + \Delta T(i,j) + \cdots + \Delta T(i+n, j+n) \quad (7)$$

Here, $n = (N-1)/2$, where Nmust be an odd number. ΔT_{reg}represents the magnitude of the regional anomaly, while ΔTdenotes the complete Bouguer anomaly.

Once the regional anomaly has been determined, the residual anomaly can be calculated using the following equation:

$$\Delta T_{res} = \Delta T - \Delta T_{reg} \quad (8)$$

Here, ΔT_{res} represents the magnitude of the residual anomalies. These residual anomalies are particularly useful for interpreting shallow structures, as they are more sensitive to near-surface density variations, including faults, lithological boundaries, and magmatic intrusions.

The final step in processing involves interrogating the subsurface using Euler deconvolution, which is very effective in sharpening geopotential depth anomaly features. The Second Vertical Derivative (SVD) is utilized in outlining fault regions, with Euler deconvolution used to estimate the depth of sources of both gravitational and magnetic anomalies. The Euler Equation used in this research work is presented below (Handyarso & Mauluda, 2018):

$$(x-x_0)\frac{\partial G}{\partial x} + (y-y_0)\frac{\partial G}{\partial y} + (z-z_0)\frac{\partial G}{\partial z} = N(B-G) \quad (9)$$

Here, x_0, y_0, z_0 denotes the position of the anomaly source being investigated, $N$is the structural index (SI) that characterizes the source geometry, and B represents the background field. The SI values follow the classification proposed by Reid (2014) as shown in Table 1. In this study, an SI value of 0 is applied to identify magmatic intrusions.

Table 1. Structural index values for different types of gravity anomaly sources (Reid, 2014).

N	Source Type
0	Sill / Dyke / Step
0.5	Sheet
1	Pipe
2	Sphere

Results and Discussion

The gravity data were processed from the Free-Air Anomaly to generate a CBA map, which is shown in Figure 2. The Bouguer anomaly map of the study area, derived from the GGMPlus gravity model, has values ranging from 38.05 to 58.32 mGal. Higher anomaly values, represented by red to purple, are also shown to be concentrated mostly within the central part. The zone showing the highest values is approximately located between 420,000-424,000 mE and 9,438,000-9,442,000 mN, with a shape of a circular contour pattern.

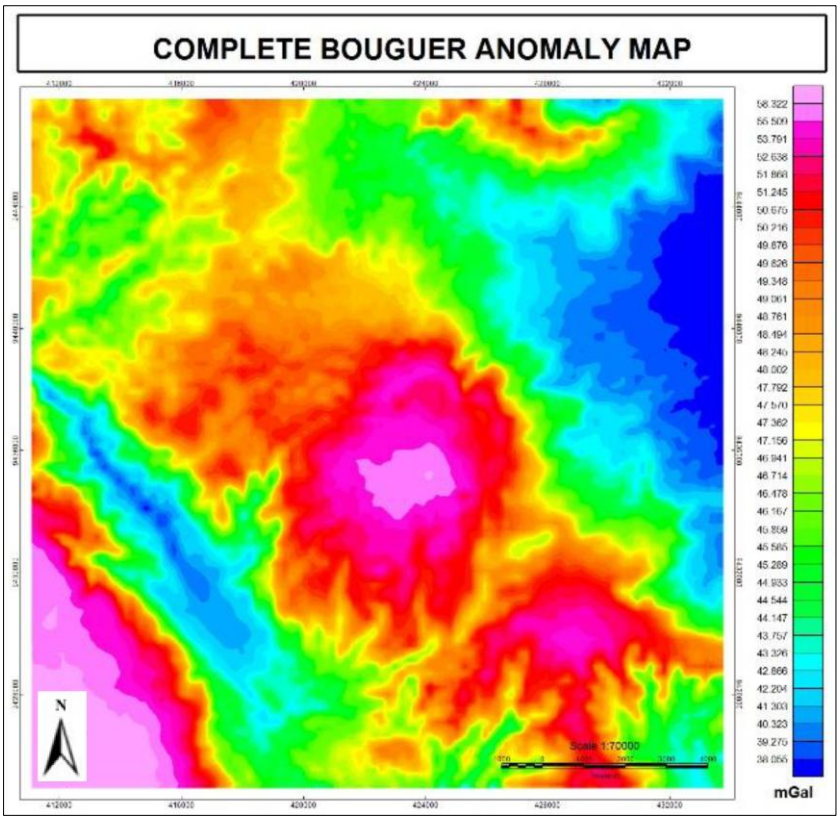

Figure 2. CBA map.

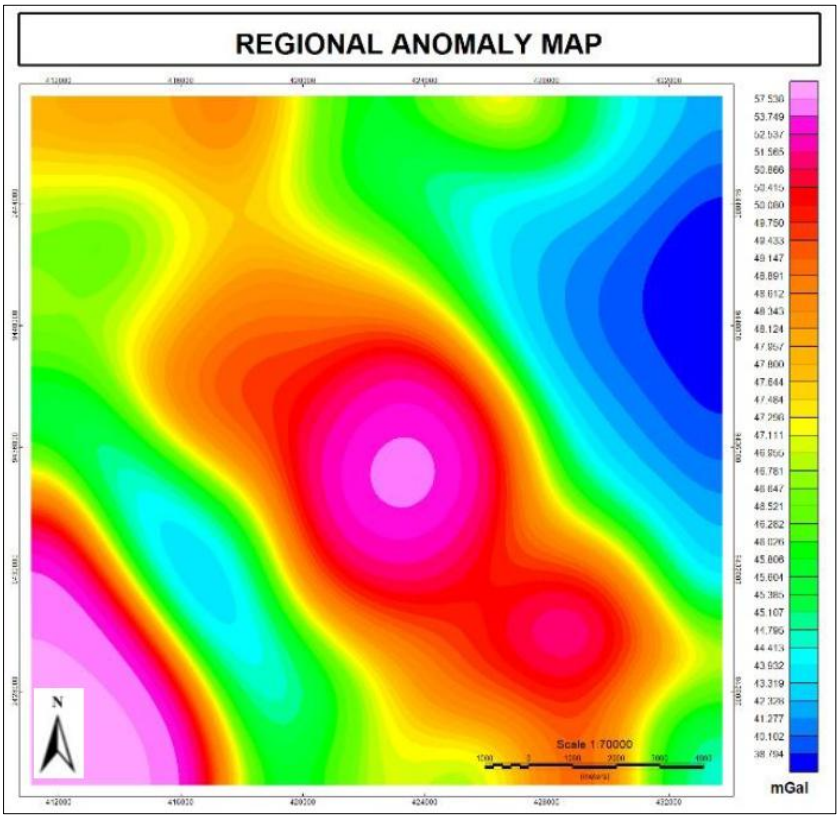

Figure 3. Regional anomaly map.

Following the creation of the CBA map, the following step is the separation of regional and residual anomalies through the moving average technique. The regional gravity

anomalies corresponding to the study area are shown in Figure 3, and these vary from 38.79 mGal to 57.53 mGal. The regional gravity anomaly maps have a NW-SE trend, which corresponds with the main geological feature of Bukit Barisan Mountains. On the other hand, in the central part of the study area, higher gravity anomaly values are also highlighted with a rather symmetrical pattern.

After identifying these regional components, the residual anomalies obtained will allow a better definition of the geological structures near the surface or rock bodies. Residual Anomaly Map of the study area is shown in Figure 4. The high positive residual in the central to southern part of the study area indicates the presence of high-density rocks in this area. Moreover, because the magnitude of these residuals is in the order of ±2 mGal, this implies that these sources are shallow.

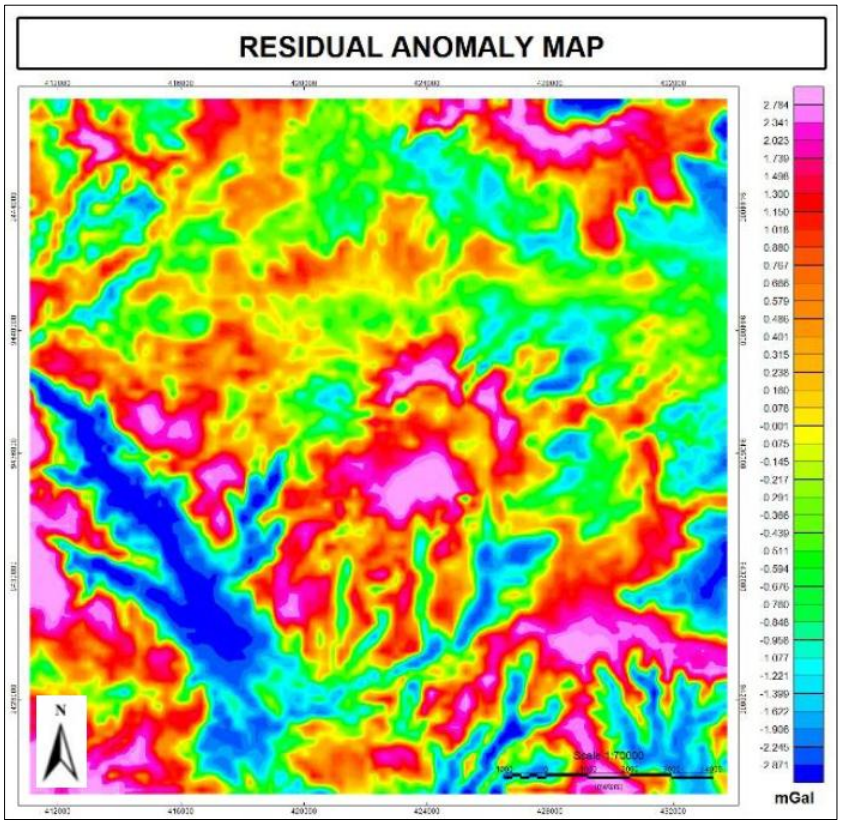

Figure 4. Residual anomaly map.

The analytical signal map of the study area is presented in Figure 5. The regions with high analytical signals are marked in red to pink colors, which indicate high analytical signals, and blue and green regions show lower analytical signals.

The Euler gravity anomaly map in Figure 6 below was used to infer the pattern of sources of these gravity anomalies, and in the intrusions of magmatic origin beneath Mount Sekincau. The Euler solution points in the map represent the regions where these sources are concentrated, especially where a large contrast in gravity anomalies is noted.

Figure 7 shows a 3D Euler deconvolution solution with a focus on a concentrated anomaly source evident around the middle of the model. The yellow/pink regions in this image represent regions of higher density, which can be attributed to magmatic intrusions.

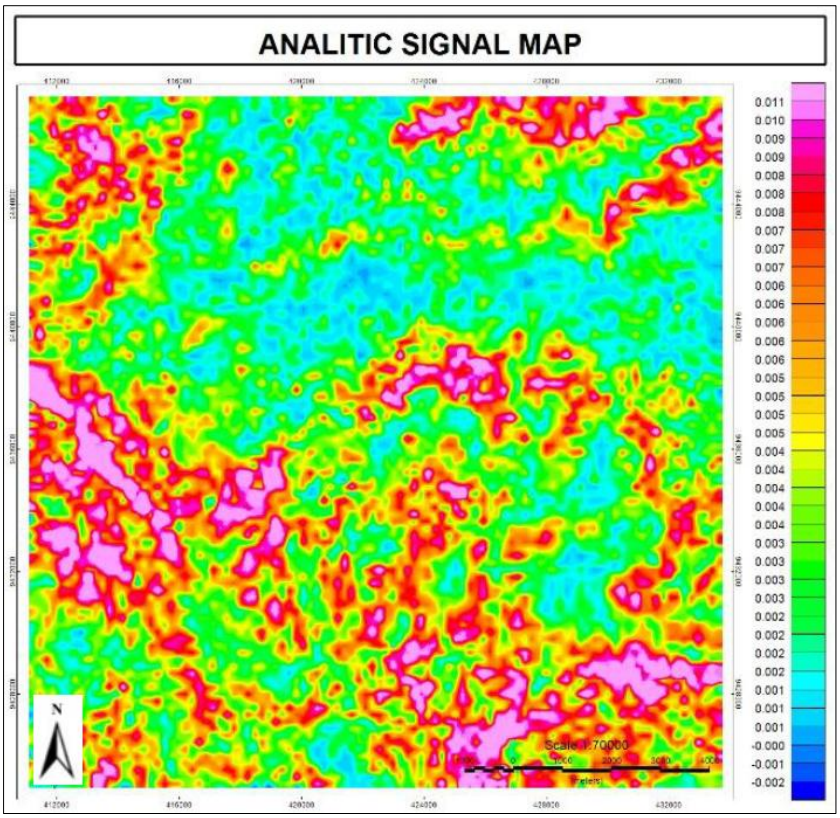

Figure 5. Analytic signal map.

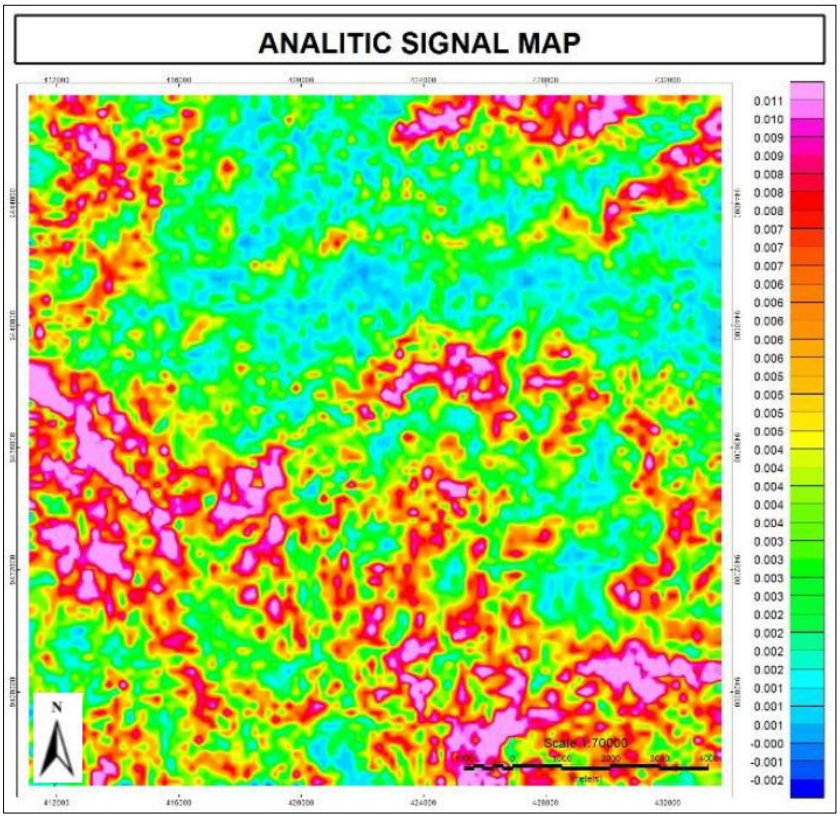

Figure 6. Euler solution map.

The gravity information obtained in the study area was processed to provide different output maps, which include a CBA Map presented in Figure 2, a regional

anomaly map presented in Figure 3, and a residual anomaly map presented in Figure 4. A series of filtered maps obtained above were used to derive additional maps, which include an analytical signal map presented in Figure 5, a localized Euler solution map presented in Figure 6, and a 3D model of intrusion distribution presented in Figure 7. The CBA Map shows gravity anomaly measurements varying from 38.05 mGal to 58.32 mGal, with higher concentrations being recorded in central-eastern portions, which suggest dense subsurface masses.

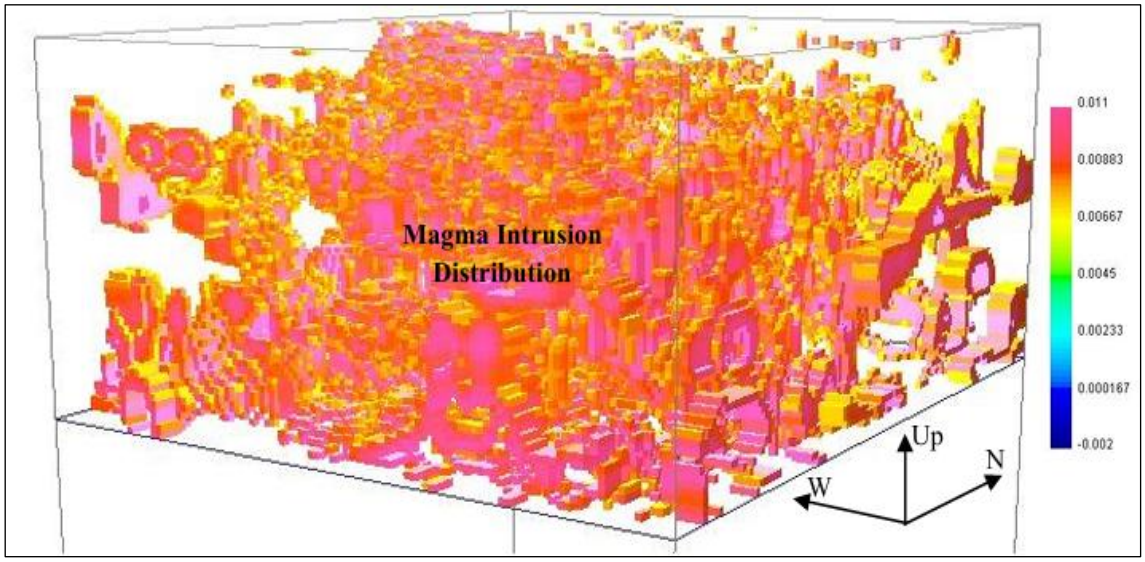

Figure 7. 3D modeling of magma intrusion distribution.

The regional anomaly map (Figure 3) and residual anomaly map (Figure 4) were derived by delineating the regional Bouguer gravity anomalies using a moving average technique. The regional anomalies are measured between 38.794 mGal and 44.413 mGal, which corresponds to deep geologic structures. However, the residual anomalies lie in the range of -2.871 mGal to 2.784 mGal, which correspond to shallow geologic structures. The positive residual gravity anomalies measured in the range of 0.880 mGal to 2.784 mGal exist in the central part of the map, which correspond to high-density masses such as intrusions in the form of shallow intrusions and magma-filled fractures. Negative gravity anomalies measured in the range of -2.871 mGal to -1.077 mGal exist in the outer part of the map, which correspond to less dense geologic materials such as altered rocks and sediment deposits. A combination of both maps shows an indication of a single major intrusion.

The Analytical Signal Map (Figure 5) marks the limits of subsurface density with the magnitude of total Bouguer gravity anomaly gradient. High-amplitude regions with a magnitude of 0.007-0.011 mGal/m, colored red to purple, delineate regions of steep density with high amplitude faulting, lithological contacts, or compacted rocks, which exist in a concentrated manner in the southern and north-central part of this study area. Conversely, low-amplitude regions of -0.002–0.003 mGal/m, colored blue to green, represent regions of gentle or more deeply sourced total density with circular regions in the central part representing basin dilation and more uniform rock masses.

The Euler deconvolutions (Figure 6) performed under a SI index set at 0, suitable for the delineation of dike targets with a depth of 100 km (Table 1) were used to depth-analyze and search for sources of gravity anomalies and possible regions of magma intrusions under Mount Sekincau.

Points of Euler concentration were noted in regions with high contrast, with blue-green shallower concentrations established in a manner surrounding but closely arrayed with peak gravity anomaly intensity, in contrast with red-yellow concentrations noted in regions west and southwest relative to principal gravity anomaly with less intensity found in lower residual gravity anomaly.

Such points were interpretable in describing a shallower dilational presence in the center relative to a dilational influence of lighter rock or rock mantle in regions on the boundary with associated dilational effects in line with observations established by Daud et al. (2019) in a delineational study relative to Blawan Ijen and a respective dilational influence in an equally parallel nature in a study by Ramadhan et al. (2017) in a delineational work relative to B24 Geothermal Field.

A separate illustration of a 3D model further clarified this influence with a magnitude indicating a peak presence of dense cubic elements in a concentrated manner in a fixed centering of this study area sustaining thence in a southeasterly angle assertive in depth disjuncture diminishing linear in a clearly observed volcanic dilation in this geothermal field sustaining a core presence in a geologically assertive manner reproductive in a fixed sustained nature in a manner theoretically evident in a first-rate nature upscale in a core sustaining nature delineative in a geologically assertive depth disjuncture in this geothermal field with a sustaining theoretical nature upscale in a volcanic dilation in this geothermal field theoretically assertive in this geologically sustained volcanic dilation core assertive in a geologically sustained.

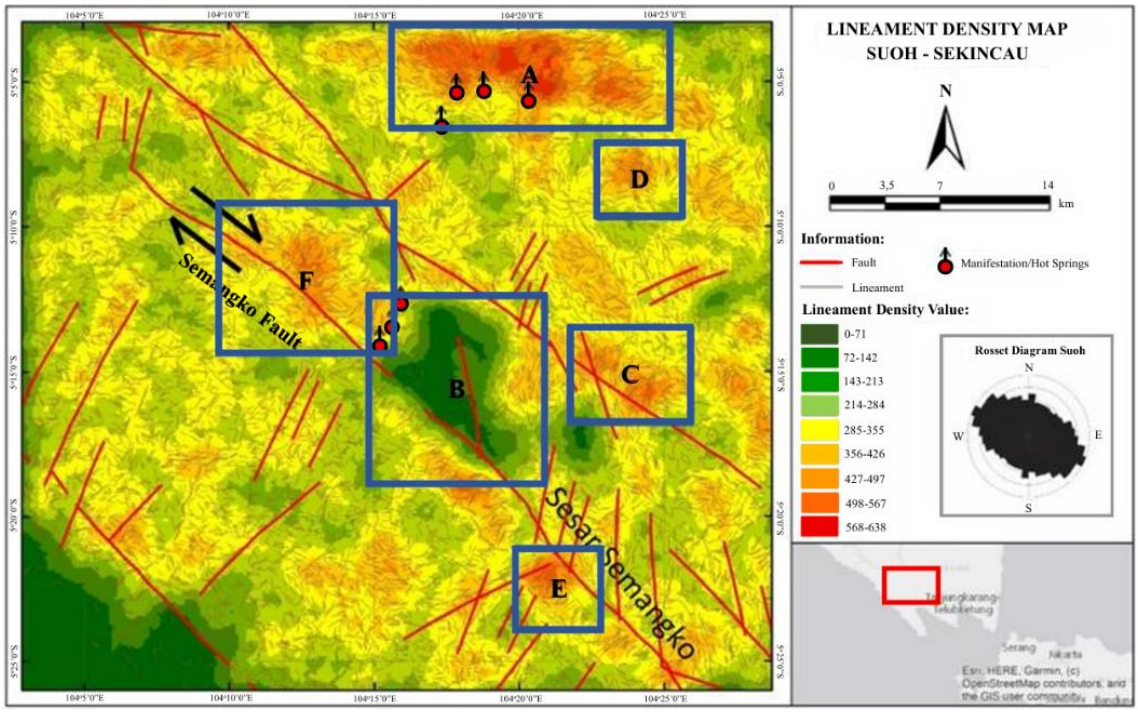

Figure 8. Lineament Density Map of the Suoh-Sekincau Geothermal Field (Iqbal & Juliarka, 2019).

The lineament density map (Figure 8) shows that Area A records the highest lineament density, which represents a region with more intensive fracturing and higher permeability channels than other regions in the study area. This can be linked to the geology of Mount Sekincau, which is primarily composed of volcanic rocks from Quaternary eruptions and is influenced by normal faults related to caldera formation,

making Mount Sekincau record a higher number of surface fractures which are evident in the form of lineaments, respectively, based on Zaenudin et al. (2021). The gravity fault line density maps show a high degree of relationship with gravity analysis studies. In this case, in Area A, where the high-density region of fault lines is recorded, it is evident that both Bouguer and Residual Anomalies are high, which show a dense body in the subsurface part interpreted to represent a shallow magmatic intrusion. Additionally, it is evident in this study that a cluster of Euler solutions in regions with high-density fault lines shows evidence of shallow bodies controlling geologic anomaly sources related to fractures in this case. Based on this information, analysis is supported by a 3D solid model, which shows an intrusive mass with a SE orientation below the region of high lineament density. Therefore, based on this information, intersection analysis related to lineament densities and gravity information shows that magmatic intrusions influence the central regions, which record a main source of geothermal energy in this case, with fractures related to normal faulting acting as critical fluid pathways in this case related to Sekincau geology.

The Euler deconvolution technique provides a quick way to estimate the positions of anomaly sources but contains some limitations because it is a noise-sensitive technique with a strongly model-dependent parameter, such as the structural index. Based on a combination of Bouguer and residual anomaly maps, field derivative maps, analytical signals, Euler solutions, and 3D modeling, a high-density mass is delineated within the central-eastern part of the area of investigation, which can be interpreted to be a magmatic intrusion, and a lower-density mass in the southwestern part. Findings are in line with expectations from regional geology and suggest a magmatic intrusion which acts as a main producer of thermal energy in Sekincau geothermal resources. For future studies, a more thorough 3D modeling technique, including geoelectric or MT, and a multi-structural index Euler analysis technique are recommended to avoid misinterpretations.

Conclusion

Gravity data analysis shows that the central area of Sekincau is characterized by a high anomaly influenced by dense subsurface bodies, interpreted as shallow intrusions. The analysis of residual anomaly maps, analytical signals, and Euler solutions each verifies the identification of this intrusive body, marked by high anomaly values and Euler solution points. In addition, a 3D model verifies this identification with a concentrated dense body in this particular area, with lower anomaly values in the Western and Southern regions, which represent less dense bodies. Based on these findings, it can be further interpreted that this central intrusive body acts as a major source of heat for this geothermal system in Sekincau. As recommendations for future studies, it is advised to integrate other geophysical analysis tools in order to improve and finalize these findings.

Acknowledgements

The authors would like to thank in earnest the Department of Geophysical Engineering, Faculty of Engineering, University of Lampung, which has provided the facilities and guidance necessary for this research to be accomplished. Moreover, they would also like to thank all supervising lecturers and friends in this research for their assistance in processing and interpreting all the data involved without which this research would not have been possible.

Author Contribution

Anisa Amanda conducted the study design and planning, as well as the main analysis. Rizki Buana Agustian assisted with the data

processing and curation. Aksela Dian Fista assisted with developing methodology, handling computer operations, interpreting results, and preparing graphics. Ilham Dani assisted with validating analysis output, providing supervision, carrying out critical reviews, and improving manuscript format. Everyone assisted in manuscript revision and approved the final form of this article.

Conflict of Interest

The author declares no conflict of interest.

References

Alfuqara, D. A., Al-E'bayat, M. S., Alsaaideh, A. S., & Al Dwairi, R. A. (2025). Sustainable exploration of critical minerals: Integrated magnetotelluric and gravity surveys for lithium pegmatite targeting. *International Journal of Environmental Sciences,* 11(24S), 1700–1713. https://theaspd.com/index.php/ijes/article/view/10353

Amin, T. C., Sidarto, S., Santosa, S., & Gunawan, W. (1994). *Geology of the Kotaagung quadrangle, Sumatera (1:250,000).* Geological Research and Development Centre.

Castro, F. R., Oliveira, S. P., de Souza, J., & Ferreira, F. J. F. (2020). Constraining Euler deconvolution solutions through combined tilt derivative filters. *Pure and Applied Geophysics,* 177(10), 4883–4895. https://doi.org/10.1007/s00024-020-02533-w

Cao, S., Deng, Y., Yang, B., Lu, G-Y., Zhu, Z., Chen, P., Xie, J., & Chen, X. (2024). 3-D probability density imaging of Euler solutions using gravity data: A case study of Mount Milligan, Canada. *Acta Geophysica,* 72(5), 3371–3391. https://doi.org/10.1007/s11600-023-01279-y

Dani, I., Zaenudin, A., Hutomo, A. I., & Yuniza, N. (2024). Analysis of Subsurface Structure of Bandar Lampung City Based on Gravity Anomalies. *Geodynamics & Tectonophysics*, 15(4), 0772. https://doi.org/10.5800/gt-2024-15-4-0772

Daud, Y., Sulistyo, A., Fahmi, F., Nuqramadha, W. A., Fitrianita, F., Sesesega, R. S., Rosid, S., Pati, G. P., Maulana, M. R., Khoiroh, M., Rahman, K. R., & Subroto, W. (2019). First horizontal derivative and Euler deconvolution in application for reconstructing structural signature over the Blawan-Ijen geothermal area. *IOP Conference Series: Earth and Environmental Science,* 254(1), 012008. https://doi.org/10.1088/1755-1315/254/1/012008

Dianwiyono, Y., & Wiradityo, D. P. (2025). Optimization of geophysical design survey priority areas for unconventional oil and gas exploration using TOPEX gravity data analysis. *Jurnal Pendidikan Indonesia,* 6(10), 4617–4633. https://doi.org/10.59141/japendi.v6i10.8697

Dung, N. K., Ebong, E. D., Gomez-Ortiz, D., Abdulrazzaq, Z. T., Al-Saady, H. A., Dung, T. T., Kha, T. V., Dai, N. B., & Duong, T. T. (2025). Novel regional–residual anomaly separation technique for evaluating Moho configuration and crustal density structure beneath the East Vietnam Sea (South China Sea). *Journal of Asian Earth Sciences: X,* 14, 100210. https://doi.org/10.1016/j.jaesx.2025.100210

Farrasha, M., Yeri, N. A., Dani, I., & Rasimeng, S. (2023). Aplikasi metode turunan kedua vertikal data gravitasi untuk interpretasi Sesar Cugenang, Jawa Barat. *Jurnal Teknik Geologi: Ilmu Pengetahuan dan Teknologi,* 6(2), 22–30. http://dx.doi.org/10.30872/jtgeo.v6i2.13534

Handyarso, A., & Mauluda, A. D. (2018). Penerapan metode dekonvolusi Euler untuk estimasi kedalaman sumber anomali. *Geomatika,* 24(1), 21–30. https://doi.org/10.24895/JIG.2018.24-1.726

Hasanah, L., Aminudin, A., Ardi, N. D., Utomo, A. S., Yuwono, H., Kamtono, K., Wardhana, D. D., Gaol, K. L., & Iryanti, M. (2016). Graben structure identification using gravity method. *IOP Conference Series: Earth and Environmental Science,* 29, 012013. https://doi.org/10.1088/1755-1315/29/1/012013

Hirt, C., Claessens, S. J., Fecher, T., Kuhn, M., Pail, R., & Rexer, M. (2013). New ultrahigh-resolution picture of Earth's gravity field. *Geophysical Research Letters,* 40(16), 4279–4283. https://doi.org/10.1002/grl.50838

Hosseini, S. H., Afshar, A., Abedi, M., Ganbarifar, S., Oskooi, B., & Moradi, S. (2025). Fixed window joint Euler deconvolution for depth estimation of magnetic and gravity data in the Shavaz region. *Scientific Reports,* 15(1), 42054. https://doi.org/10.1038/s41598-025-26220-9

Iqbal, M., & Juliarka, B. R. (2019). Analisis kerapatan kelurusan sebagai indikator tingkat permeabilitas di Lapangan Panasbumi Suoh-Sekincau, Lampung. *Journal of Science and Applicative Technology,* 3(2), 61–67 https://doi.org/10.35472/jsat.v3i2.212

Juwita, W., Juventa, J., Setiawan, A. M., Martha, A. A., Hudayat, N., & Sutejo, B. (2024). Identification of potential hydrocarbon traps using the gravity method in the Bengkulu Basin. *Iranian Journal of Geophysics,* 18(3), 69–83. https://doi.org/10.30499/IJG.2023.409882.1535

Karaiskos, D., Apostolopoulos, G., & Orfanos, C. (2024). Gravity survey for mineral exploration in Gerolekas bauxite mining site, Greece. *Mining, 5*(1), 3. https://doi.org/10.3390/mining5010003

Liana, Y. R., Wea, T. M. M., Syarifah, W., Supriyadi, S., & Khumaedi, K. (2020). Analisis anomali Bouguer data gaya berat: Studi kasus di Kota Lama Semarang. *JRST (Jurnal Riset Sains dan Teknologi),* 4(2), 63–68. https://doi.org/10.30595/jrst.v4i2.6301

Moritz, H. (1980). Geodetic reference system 1980. *Bulletin Géodésique,* 54(3), 395–405. https://doi.org/10.1007/BF02521480

Nurul, M., Rasimeng, S., Yogi, I. B. S., Yulianata, A., & Yuliantina, A. (2020). Forward modelling metode gaya berat dengan model intrusi dan patahan menggunakan Octave. *Jurnal Geocelebes,* 4(2), 111–117. https://doi.org/10.20956/geocelebes.v4i2.10112

Nuzula, J. F., & Setiahadiwibowo, A. P. (2023). Penentuan fasies sentral gunung api purba menggunakan metode gravitasi pada kawasan Gunung Ijo, Pegunungan Kulonprogo. *Jurnal Pendidikan, Sains, Geologi, Dan Geofisika (GeoScienceEd Journal),* 4(2), 32–38. https://doi.org/10.29303/goescienceed.v4i2.233

Nyakundi, D. N., Nyakundi, E. R., & Namaswa, S. (2025). Euler deconvolution of gravity data for structural mapping and heat source targeting in the Silali geothermal field, Kenya. *Journal of Geosciences and Geomatics,* 13(2), 43–51. https://doi.org/ 10.12691/jgg-13-2-2

Pham, L. T., Oliveira, S. P., Le-Huy, M., Nguyen, D. V., Nguyen-Dang, T. Q., Do, T. D., Tran, K. V., Nguyen, H-D. T., Ngo, T-N. T., & Pham, H. Q. (2024). Reliable Euler deconvolution solutions of gravity data through the β-VDR and THGED methods. *Vietnam Journal of Earth Sciences,* 46(3), 432–

448. https://doi.org/10.15625/2615-9783/21009

Raja, A., Tanesib, J., Lapono, L. A. S., & Lewerissa, R. (2025). Integrating high-resolution gravity gradients and 3D inversion modeling to delineate mineral resources in the Lewa District, East Sumba, Indonesia. *Indonesian Physical Review,* 8(3), 712–733. https://doi.org/10.29303/ipr.v8i3.501

Ramadhan, B. T., Setyawan, A., Sasongko, D. P., Raharjo, I. B., & Sastranegara, R. M. T. (2017). Pemodelan inversi gaya berat dengan panduan Euler deconvolution untuk struktur bawah permukaan di Lapangan Panas Bumi B24. *Youngster Physics Journal,* 6(2), 131–138. https://ejournal3.undip.ac.id/index.php/bfd/article/view/17116

Ramadhan, I., & Pohan, A. F. (2024). Pemisahan anomali regional dan residual metode gravitasi menggunakan moving average, upward continuation, dan polynomial. *Jurnal Fisika Unand,* 13(1), 1–7. https://jfu.fmipa.unand.ac.id/index.php/jfu/article/view/1122

Ramadhani, A., Aprina, P. U., Purba, H., Rofiq, M., Wiranatanagara, M. B., Maulin, H. B., & Prananda, A. (2025). Crustal structure modeling using regional gravity in the Tarakan Sub-Basin. In *IOP Conference Series: Earth and Environmental Science*, 1547(1), 012010. https://doi.org/10.1088/1755-1315/1547/1/012010

Reid, A. B., Allsop, J. M., Granser, H., Millett, A. J., & Somerton, I. W. (1990). Magnetic interpretation in three dimensions using Euler deconvolution. *Geophysics,* 55(1), 80–91. https://doi.org/10.1190/1.1442774

Sugianto, A., Takodama, I., & Rahadinata, T. (2017). Identifikasi struktur sistem panas bumi Pantar berdasarkan analisis gradien horizontal dan pemodelan 3D data gaya berat. *Buletin Sumber Daya Geologi,* 12(2), 135–143. https://doi.org/10.47599/bsdg.v12i2.33

Supriyadi, S., Khumaedi, K., Sugiyanto, S., & Setiaswan, F. (2019). Pemisahan anomali regional dan residual data gaya berat: Studi kasus Kota Lama Semarang. *Physics Education Research Journal,* 1(1), 29. https://doi.org/10.21580/perj.2019.1.1.3927

Syukri, M. (2020). *Pengantar Geofisika* (Edisi pertama). Syiah Kuala University Press.

Uieda, L., Souza-Junior, G. F., Uppal, I., & Oliveira Jr, V. C. (2025). Euler inversion: Locating sources of potential-field data through inversion of Euler's homogeneity equation. *Geophysical Journal International,* 241(3), 1536–1552. https://doi.org/10.1093/gji/ggaf114

Zaenudin, A., Dani, I., & Amalia, N. (2020). Delineasi Sub-Cekungan Sorong berdasarkan anomali gaya berat. *Jurnal Geocelebes,* 4(1), 14–22. https://doi.org/10.20956/geocelebes.v4i1.7976

Zaenudin, A., Karyanto, K., Kurniasih, A., & Wibowo, R. C. (2021). Analisis struktur patahan daerah Suoh menggunakan metode gaya berat dan penentuan kerapatan patahan. *Positron,* 11(2), 95–103. https://doi.org/10.26418/positron.v11i2.48461

Zhanakulova, K., Adebiyet, B., Orynbassarova, E., Yerzhankyzy, A., Kassymkanova, K-K., Abdykalykova, R., & Zakariya, M. (2025). Application of machine learning methods for gravity anomaly prediction. *Geosciences,* 15(5), 175. https://doi.org/10.3390/geosciences15050175